Relaxation Behaviour of Shot Peening Induced Residual Stresses in AISI 4140 due to Quasistatic Uniaxial Loading at Elevated Temperatures

H. Holzapfel, V. Schulze, O. Vöhringer, E. Macherauch
Institut für Werkstoffkunde I, Universität Karlsruhe,
Kaiserstr. 12, D 76128 Karlsruhe, FRG

ABSTRACT

The relaxation behaviour of shot peening residual stresses due to quasistatic loading was investigated for the steel AISI 4140 in a normalized and a quenched and tempered condition. For tensile or compressive loadings at room temperature, 250 °C and 400 °C the deformation behaviour of the shot peened specimens and the remaining residual stresses after unloading from several loading stress levels were determined. The critical stress for the onset of stress relaxation and the stress relaxation rate are influenced in a characteristic manner by tensile or compressive loadings and by the material state. Differences due to the temperature dependence of residual stress relaxation at the two heat treatment conditions are discussed with respect to the effect of dynamic strain ageing. Additionally, results obtained from a finite element modelling show that the thermal residual stress relaxation is only effective during heating and waiting for temperature compensation before quasistatic loading and can be completely neglected during quasistatic loading.

KEYWORDS

shot peening residual stresses, relaxation behaviour, onset of stress relaxation, quasistatic loading, dynamic strain ageing, Bauschinger-effect, finite element modelling.

INTRODUCTION

The deformation and failure behaviour of metallic materials can be influenced by residual stresses, which are generated by production or/and during operation. Thus compressive residual stresses in the surface region of materials with medium and high hardnesses increase for instance the fatigue life and the fatigue limit at cyclic loading in comparison with material states which are free of residual stresses. Thereby, the stability of these residual stresses at purely thermal or mechanical as well as superposed thermal and mechanical loadings is of decisive importance. In the case of mechanical loading, there exists in addition to cyclic loadings also an interest on quasistatic loadings, which serve as a basis for the evaluation of the cyclic residual stress relaxation in the first cycle. Whereas several investigations exist dealing with the thermal relaxation of residual stresses [1-15] as well as the quasistatic relaxation at room temperature [1,2,16-21], no systematic work is known concerning the quasistatic relaxation at higher temperatures. Therefore, in this report results of corresponding experiments and of the

modelling of the quasistatic relaxation of shot peening residual stresses are presented for the steel AISI 4140 (German grade 42CrMo4) at increased temperatures.

MATERIAL, HEAT TREATMENTS AND EXPERIMENTAL PROCEDURE

The investigations were carried out for the steel AISI 4140 (German grade 42CrMo4) with the chemical composition 0.41 C, 1.03 Cr, 0.18 Mo, 0.29 Si, 0.73 Mn, 0.19 Ni, 0.02 P, 0.02 S and the rest Fe (all in wt.-%). Round specimens with a gauge length of 10 mm and a diameter of 7 mm were produced and heat treated in a vacuum quenching furnace. The specimens of the normalized condition were austenitized at 930°C for 3h and slowly cooled down in the furnace. The quenched and tempered condition (T450) was produced by austenitizing for 20min at 850°C, oil quenching down to 25°C, tempering at 450°C for 2h and finally slow cooling in the furnace. The shot peening was performed in an air blast machine with cast steel shot S 170 (mean diameter 0.43 mm) of 46 HRC hardness. A pressure of 1.6 bar and a flow rate of 1.5 kg/min resulted in a coverage of 98 %. A universal 100 kN-testing machine was used for the tension and compression tests. All specimens were deformed with a strain rate of $\dot{\varepsilon} = 4 \cdot 10^{-4}\,s^{-1}$ using special equipments [22]. Before and after each experiment the surface residual stresses and the half width breaths of the shot peened specimens were measured in the direction of the specimen axis using the X-ray technique. The determination of the residual stresses was achieved thereby with CrKα-radiation at the {211}-interference lines of each specimen at 11 Ψ-angles between -45° and +45° according to the $\sin^2\text{-}\Psi$ method [23]. The determination of the depth distributions of the residual stresses was performed by an iterative electrolytical removal of thin surface layers and subsequent X-ray measurements. These residual stress values were corrected according to the surface removal [24].

MODELLING AND INPUT DATA

Finite-element calculations of the relaxation of residual stresses due to quasistatic loading were carried out with the program ABAQUS. Assuming plane residual stress distributions in the shot peened surface layers, the really existing three-dimensional problem can be reduced to a two-dimensional one.Thereby, the cross-section of a rectangular flat specimen is subdivided in sufficiently small orthogonal elements, which allow a good discretization of the residual stress distribution as well as the workhardening behaviour. (A rectangular cross-section was used with nearly the same ratio of shot peening influenced area to total cross-section area, because of the reduction of the expenditure of calculations). The element type consists of a isoparametric model with 8 nodes on the border and 9 integration points in the interior of the elements under plane strain conditions. For the calculation of the residual stress relaxation the implementation of the initial residual stresses and the workhardening curves for each layer is necessary. At higher temperatures the thermal residual stress relaxation due to heating and waiting for temperature compensation is also taken into account in the input data.

EXPERIMENTAL RESULTS

Characterization of the shot peened surface layers

The depth distributions of the residual stresses and the half width breaths after the shot peening of both heat treatment conditions are represented in Fig. 1. In the normalized condition the magnitudes of residual stresses (Fig. 1a) decrease continuously until reaching the core material. In a depth of 0.3 mm the transition from compressive to tensile residual stresses occurs, which is caused by the equilibrium condition. In the quenched and tempered condition the residual stresses assume a value of -600 N/mm² and remain nearly constant to a depth of 0.15 mm. Then the magnitude of the residual stresses rapidly decrease up to zero at 0.225 mm (Fig.1a). While the half width breaths of the diffracted interference lines in the surface region of the normalized specimens increased from 2.0 °2θ to 2.7 °2θ as a result of shot peening, no significant change of the half width breaths of about 3.2 °2θ was observed for the quenched and tempered specimens (Fig. 1b).

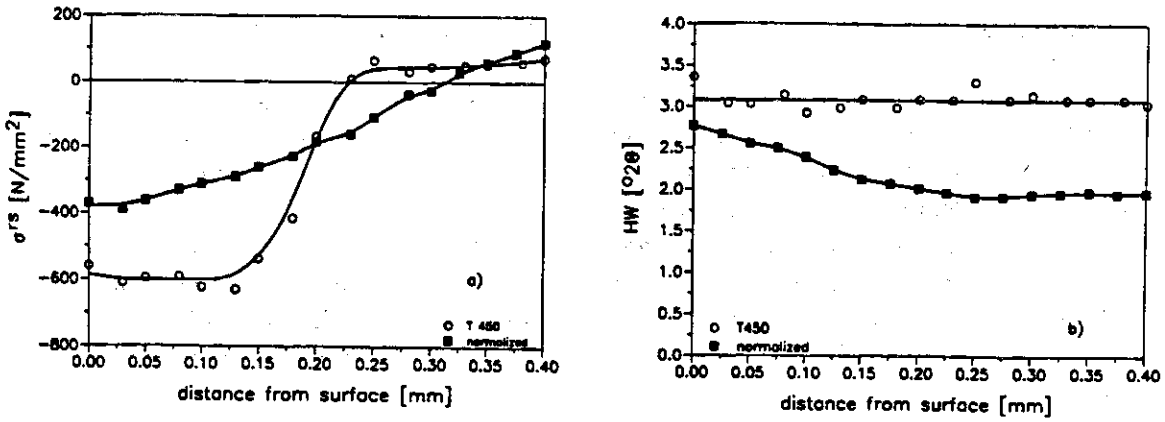

Fig. 1: Residual stress σ^{rs} and half width breath HW versus distance from surface. a) Normalized condition, b) quenched and tempered condition (T450)

Normalized condition

The behaviour of the shot peening residual stresses σ^{rs} in dependence of the loading stress σ^{L} for tensile and compressive loading at temperatures of 25°C, 250°C and 400°C is presented in Fig. 2a. The data points at 250°C and 400°C for σ^{L} = 0 N/mm² correspond to the residual stresses, which were measured by heating and waiting for compensation of the temperature between surface and core of the specimens before loading. The residual stress relaxation at 25°C starts during tension at the critical loading stress σ^{L}_{crit} = 300 N/mm² [18]. Then the relaxation intensifies itself rapidly with increasing load. Moreover, at sufficiently high tensile loading stresses even tensile residual stresses are generated. The residual stress relaxation during compressive loading begins at $\sigma^{L}_{crit} \approx$ -300 N/mm². An increase of the stress up to σ^{L} = -750 N/mm² leads to a complete relaxation of the residual stresses. Since the specimens, which were tested at 250°C and 400°C, are characterized by larger magnitudes of the initial residual stresses directly after shot peening than those, which were tested at 25°C ($\sigma^{rs} \approx$ -340 N/mm² and $\sigma^{rs} \approx$ -280 N/mm², resp. [25]), no significant differences occur between the residual

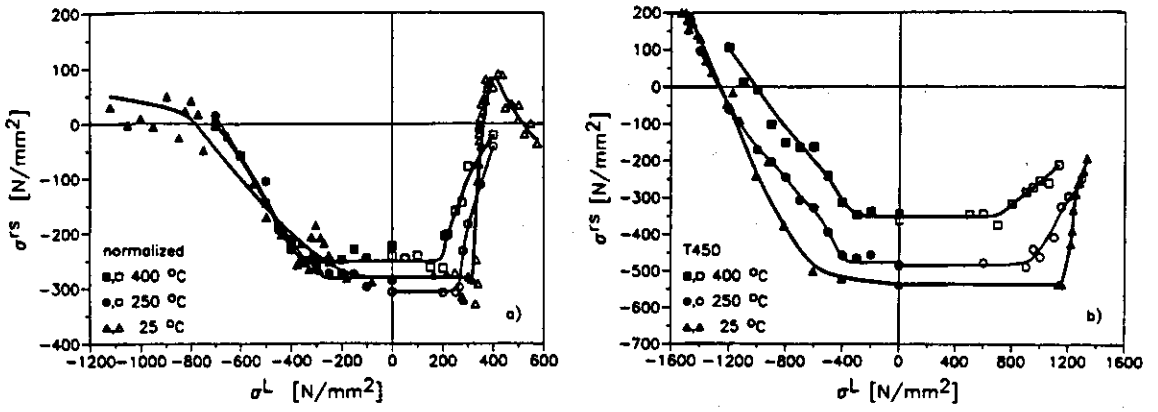

Fig. 2: Residual stress σ^{rs} vs. loading stress σ^{L} at different deformation temperatures. a) Normalized condition, b) quenched and tempered condition (T450)

stresses at 25°C and 250°C for σ^{L} = 0 N/mm². However, under the same material and shot peening conditions the initial residual stresses are relaxed after heating up and waiting for temperature compensation about 15% at 250°C and about 30% at 400°C [25]. With increasing deformation temperature the critical tensile loading stress at which the residual stress relaxation starts is reduced (see also Fig. 3). At 250°C and 400°C the further residual stress relaxation proceeds slowlier than at room temperature. All data points at compressive loading lie closely together. The value of the critical compressive loading stress σ^{L}_{crit} = -400 N/mm² at 400°C, which characterizes the onset of residual stress relaxation, is slightly larger than the corresponding value for room temperature (Fig. 3).

Quenched and tempered condition

Fig. 2b illustrates the influence of loading stresses on the shot peening residual stresses σ^{rs} for the different testing temperatures. During tensile loading at 25°C the onset of residual stress relaxation occurs at σ^{L} = 1150 N/mm². Though the relaxation rate at increasing loading stresses is very high, no complete relaxation of the compressive residual stresses is observed. Compressive loading stresses with a magnitude larger than 600 N/mm² lead to residual stress relaxation. Furthermore at very large compressive loading stresses tensile residual stresses are measured. At higher temperatures

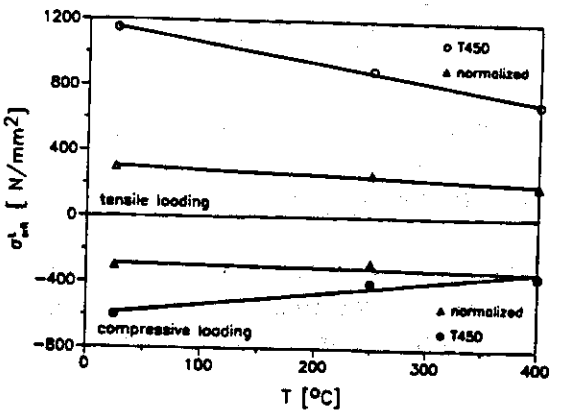

Fig. 3: Critical loading stress σ^{L}_{crit} for the onset of residual stress relaxation vs. temperature T in the normalized and quenched and tempered conditions

the residual stresses are characterized qualitatively by the same behaviour as in the normalized condition. However, the initial residual stresses are clearly reduced by heating and waiting for temperature compensation at 250°C and 400°C. Both values of the critical loading stresses for the onset of residual stress relaxation during tension and compression decrease clearly with increasing temperature (see also Fig. 3). The relaxation rate is also reduced with increasing temperature.

DISCUSSION

Critical loading stresses and relaxation rates

In general residual stress relaxation starts, if the sum of loading and residual stresses exceeds the local resistance to plastic deformation, the yield strength $R_{e(t)}$ during tension or $R_{e(c)}$ during compression. In the case of tensile loadings, this means that the sum of critical loading stress σ^L_{crit} and maximum tensile residual stress in the specimen core σ^{rs}_C attains the yield strength of the core $R_{e(t),C}$. However, during compressive loadings the sum of the magnitudes of σ^L_{crit} and maximum compressive residual stresses of the surface region σ^{rs}_S must reach the surface yield strength $R_{e(c),S}$. Consequently, under uniaxial consideration, the following relationships are valid for tensile loading

$$R_{e(t),C} = \sigma^L_{crit} + \sigma^{rs}_C \qquad (1)$$

and for compressive loading

$$|R_{e(c),S}| = |\sigma^L_{crit}| + |\sigma^{rs}_S|. \qquad (2)$$

The core yield strength under tensile loading $R_{e(t),C}$ should be identical with the yield strength $R_{e(t)}$ of the unpeened condition. On the other hand, the surface yield strength under compressive loading $R_{e(c),S}$ generally shows changed values due to the shot peening induced deformation of the surface layers. Therefore, a more exact determination of $R_{e(c),S}$ is carried out in the following, which allows more profound conclusions concerning the workhardening behaviour of the surface layers.

During the shot peening treatment a predominating biaxial residual stress state is generated with nearly identical components in longitudinal and transverse direction of the specimen axis. Residual stress relaxation starts during compressive loading, if the equivalent stress σ_{eq} reaches the magnitude of the surface yield strength $R_{e(c),S}$. Based on the v. Mises hypothesis the relationship

$$|R_{e(c),S}| = \sigma_{eq} = \sqrt{\left(\sigma^{rs}_S + \sigma^L_{crit}\right)^2 + \left(\sigma^{rs}_S\right)^2 - \left(\sigma^{rs}_S + \sigma^L_{crit}\right)\sigma^{rs}_S} \qquad (3)$$

is valid. The application of eq.(3) for both heat treatment conditions results in the $R_{e(c),S}$-values, which are summarized in Table 1. The corresponding yield strength of the unpeened conditions during compression $R_{e(c)}$ and the ratio $R_{e(c),S}/R_{e(c)}$ are also indicated in Table 1.

In the case of the normalized condition, the maximum compressive residual stress σ^{rs}_S appears directly at the surface, which is compatible with the experimental findings in Fig. 1. In this condition, obviously the shot peening treatment leads to surface yield

Table 1: Yield strength $R_{e(c)}$, surface yield strength $R_{e(c),S}$ and yield strength ratio $R_{e(c),S}/R_{e(c)}$ of AISI 4140 in different heat treatment conditions

heat treatment	yield strength	temperature		
		25°C	250°C	400°C
normalized	$R_{e(c)}$ [N/mm²]	-345	-300	-275
	$R_{e(c),S}$ [N/mm²]	-480	-496	-516
	$R_{e(c),S}/R_{e(c)}$	1.39	1.65	1.87
quenched and tempered	$R_{e(c)}$ [N/mm²]	-1300	-950	-830
	$R_{e(c),S}$ [N/mm²]	-953	-758	-606
	$R_{e(c),S}/R_{e(c)}$	0.73	0.79	0.73

strengths at all temperatures investigated, which are larger than in the unpeened condition (Table 1). Consequently, the shot peening induced deformation produces workhardened surface layers due to locally increased dislocation densities. This finding is in agreement with the behaviour of the half width breaths as a measure of the microstructural workhardening (see Fig. 1a).

These considerations make possible to explain the temperature dependencies of the critical loading stresses of the normalized condition, which are presented in Fig. 3. During tensile loading the specimen core with its tensile residual stresses controls the behaviour of σ^L_{crit}. The decreasing values with increasing temperature mainly result from the reduced yield strength $R_{e(t)}$ with temperature (see Table 1), since in this case the thermal relaxation of the tensile residual stresses in the core is insignificant [25].

From the results in Fig. 2a it is evident that the residual stresses during tensile loading for $\sigma^L > \sigma^L_{crit}$ and higher temperatures are slowlier relaxed than at room temperature. This finding can be explained qualitatively by Fig. 4, in which the initial parts of the workhardening curves of the normalized state in the unpeened condition are presented for 25°C, 250°C and 400°C. For total strains up to ε_t = 0.8% a Lüders deformation appears at room temperature. This means for the illustration in Fig. 2a, that at a nearly constant loading stress an increasing plastic deformation results, which causes a large residual stress relaxation. Therefore, in the plot σ^{rs} vs. σ^L the residual stresses at 25°C are relaxed rapidly after reaching σ^L_{crit}. The Lüders band has disappeared nearly at 250°C and completely at 400°C. Consequently at higher temperatures in comparison

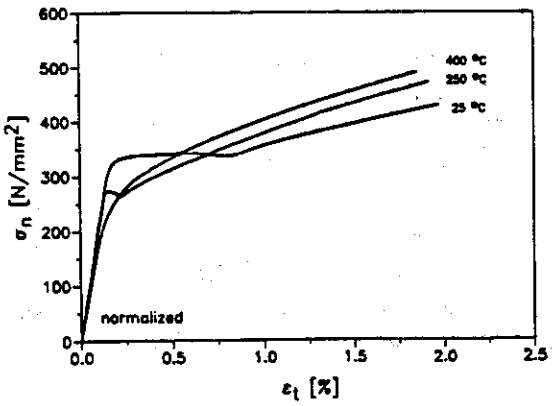

Fig. 4: Initial parts of the tensile workhardening curves of the normalized condition at different temperatures (σ_n = nominal stress, ε_t = total strain)

with room temperature a larger loading stress difference to reach a comparable plastic deformation must be brought up. This behaviour leads to smaller slopes with increasing temperature in Fig. 2a.
The magnitude of the critical loading stress $\sigma^{\perp}_{crit}$ at compressive loading increases with temperature in contrast to the loading under tension. This behaviour can be interpreted by nearly identical workhardening curves between 25°C and 400°C due to the effect of dynamic strain ageing at higher temperatures [25], where a strong elastic interaction of glide dislocations and diffusing carbon atoms occurs. Therefore nearly temperature independent surface yield strengths are expected, which agree with the results in Table 1. Since the compressive residual stresses are particularly relaxed with increasing temperature by heating and waiting for temperature compensation, larger magnitudes of the critical loading stresses can be brought up at higher temperatures until the mechanical residual stress relaxation starts.
At further increase of the loading stress values during compression $|\sigma^{\perp}| > |\sigma^{\perp}_{crit}|$, the data points for all temperatures practically coincide. This behaviour is again a consequence of the dynamic strain ageing, which induces insignificant differences in the compressive workhardening curves at 25°C, 250°C and 400°C [25].
At the quenched and tempered condition T450 completely other relationships appear. As can be seen from Fig. 3, the magnitudes of $\sigma^{\perp}_{crit}$ decrease with increasing temperature during tensile as well as compressive loadings. The surface yield strength $R_{e(c),S}$, which was determined with eq. (3), decreases with temperature in an analogous manner as the compressive yield strength of the unpeened condition (see Table 1). Consequently the ratio $R_{e(c),S}/R_{e(c)}$ is temperature independent. Moreover, the ratio is smaller than 1 due to a shot peening induced worksoftening of the surface layer. It is obvious that this finding is the consequence of the Bauschinger-effect, which occurs in the surface layer - with a stronger intensity than in the normalized condition [27] - during compressive loading after the shot peening induced biaxial tensile deformation of this surface layer. The dynamic strain ageing process, which was mentioned in this context for the normalized condition, can also have an influence on these properties in the T450 condition. However, the consequences of this effect are considerably reduced due to significantly higher dislocation densities in this condition. The resulting worksoftening effect is compatible with the behaviour of the half width breaths in Fig. 1a, where the shot peening induced increase of the dislocation density and the rearrangements and annihilations of dislocations during shot peening are balanced. The half width breaths, which do not change significantly with increasing distance from surface, indicate, that the dislocation density is significantly higher than in the normalized condition. However, the mobility of the dislocations in the deformed surface layer is anisotropic and different according to loadings in tension or compreesion due to the Bauschinger-effect.
In the case of tensile loading the explanation of the temperature dependency of $\sigma^{\perp}_{crit}$ and of the residual stress relaxation rate is in principle the same as for the normalized condition. $\sigma^{\perp}_{crit}$ decreases with increasing temperature because the yield strength $R_{e(t),C}$ is reduced more intensely than the residual stresses σ^{rs}_{C} due to heating and waiting for temperature compensation. In an analogous manner as for the normalized condition at room temperature the largest residual stress relaxation rate is observed due to a smaller workhardening effect for $\varepsilon_t \leq 1\%$ than at 250°C and 400°C [25]. In contrast to the normalized condition, the magnitude of $\sigma^{\perp}_{crit}$ under compressive loading decreases considerably with temperature. Obviously, the distinctive temperature dependence of

the workhardening curves during compression causes the large reduction of the surface yield strength $R_{e(c),S}$. The higher value of the relaxation rate can be caused by the assumption of a surface workhardening curve, which is smoother than the curves at higher temperatures. However, a more exact discussion of this behaviour is only possible by the aid of the FE-modelling.

Modelling of the relaxation behaviour

The finite-element calculations require discretizised depth distributions of the initial residual stresses under consideration of the thermal residual stress relaxation due to heating as well as the workhardening curves at different temperatures, loadings and heat treatment conditions for each surface layer. The implementation of the workhardening curves will be described exemplarily by means of the curves under compression at room temperature. In both heat treatment conditions the workhardening curves for the specimen core were based on data from compression tests of unpeened states. However, the assumptions with reference to the workhardening curves of the surface layers take into account the characteristic workhardening behaviour of the materials, which differs for both conditions.

The construction of the surface workhardening curves in the normalized condition (valid for distances from surface $\leq$ 0.2 mm) was performed with regard to the surface yield strengths $R_{e(c),S}$. In this case it is assumed, that the shot peening treatment results in a predeformation of the specimen to the stress value $\sigma = R_{e(c),S}$. After reloading in compression the assumed surface workhardening curve should flow into the original stress-strain curve of the unpeened condition at $\sigma = R_{e(c),S}$. The surface workhardening curve thus yields from the core-curve through horizontal shifting of the σ_n,ε_p-part above $R_{e(c),S}$ on the left to the point $\sigma = R_{e(c),S}$, $\varepsilon_p = 0\%$. The workhardening curve for the transition region (0.2 to 0.4 mm distance from surface) represents the arithmetical mean of surface and core behaviour. The input data for the FE-calculations are plotted in Fig. 5a, joined together by a polygon by the ABAQUS-program. The workhardening curves at tension and all curves at higher temperatures were determined in analogous manner [25].

Fig. 6a presents the comparison between the experimental results and the accomplished FE-calculations at 25°C and 400°C. In the regime $\sigma^L > 0$ a satisfactory agree-

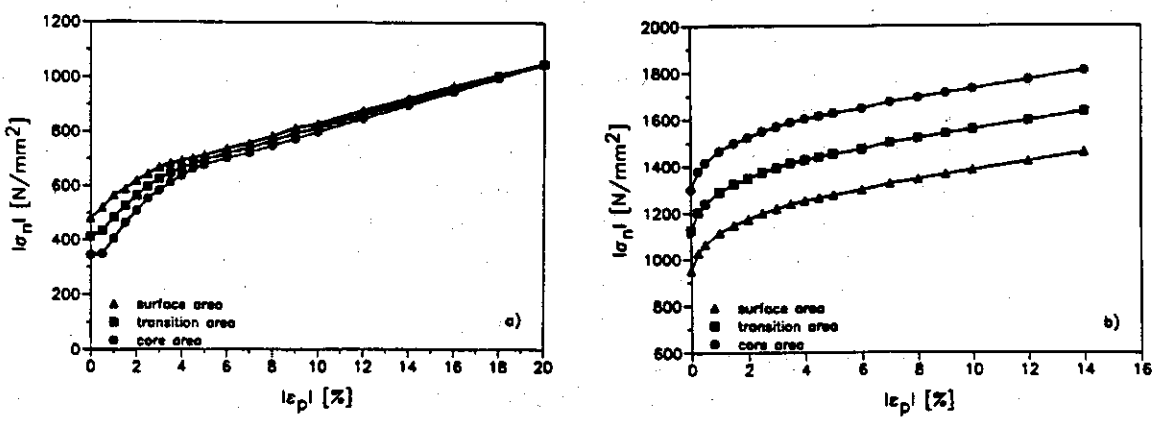

Fig. 5: Workhardening curves in compression for surface, transition and core area at room temperature. a) Normalized, b) quenched and tempered (T450)

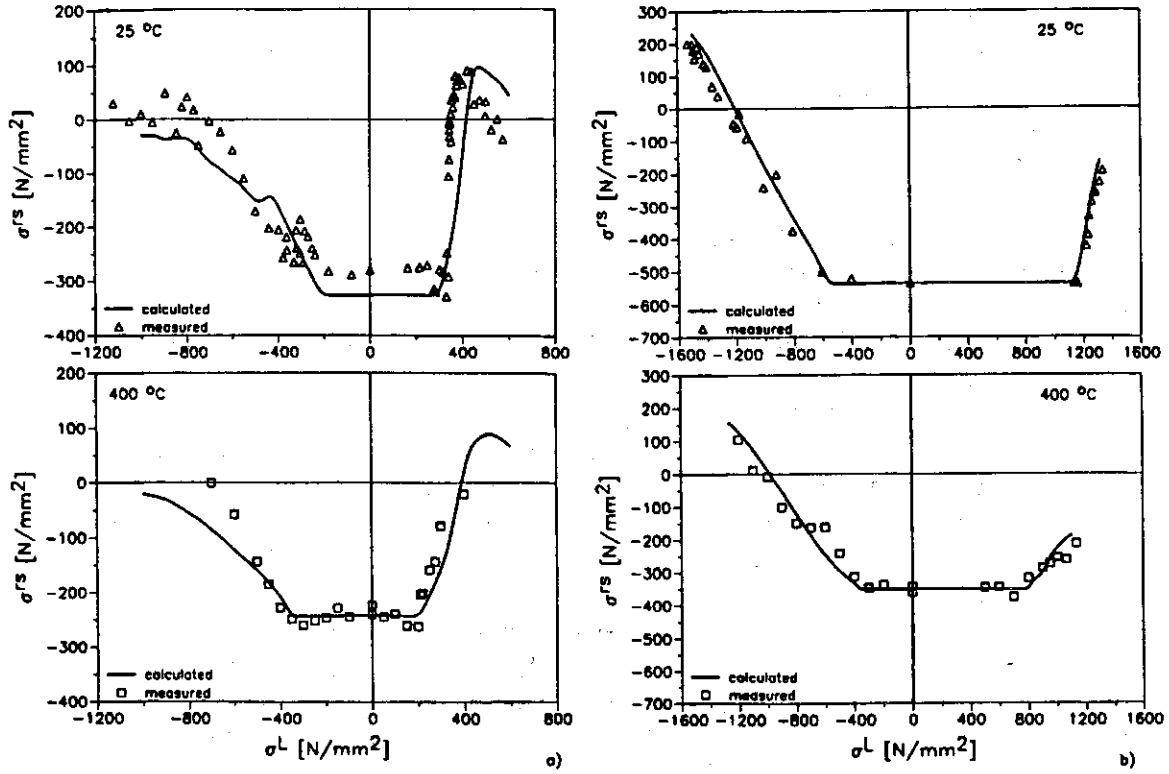

Fig. 6: Measured and calculated residual stress vs. loading stress at 25°C (at the top) and 400°C (at the bottom). a) Normalized, b) quenched and tempered (T450)

ment exists. The modelling is obviously suited to describe the onset of residual stress relaxation as well as the change of sign at larger tensile loading stresses. However, the residual stress relaxation rate is higher in the experimental results than in the calculated variant. At 400°C the results measured and modelled under tensile loading agree very well. During compressive loading the beginning of the residual stress relaxation can also be well modelled for both temperatures. With increasing magnitude of the compressive loading stresses $|\sigma^L| > |\sigma^L_{crit}|$ the modelling at first describes the measured data satisfactorily. At larger loadings, however, differences between experiment and modelling appear (Fig. 6a), and the FE-calculation cannot describe the change of sign of the residual stresses. The instability in the course at $\sigma^L \approx -400$ N/mm² can be explained by a stress incompatibility at the onset of plastic deformation in the specimen core due to Lüders deformation.

The development of workhardening curves at the quenched and tempered condition, which are shown in Fig. 5b, is based on the experimental result that in comparison to the unpeened condition after shot peening the surface yield strength $R_{e(c),S}$ decreases due to the Bauschinger-effect. Thus the surface workhardening curve (controlling the workhardening behaviour in the distance from surface $\leq$ 0.15 mm) was formed by parallel shifting of the core curve along the stress axis to lower values by the magnitude of the yield strength difference $\Delta R_e = |R_{e(c)}| - |R_{e(c),S}|$. In the transition region (0.15 to 0.30 mm distance from surface) the workhardening curve is determined analogous to the normalized condition by the mean values of the flow stresses from surface and core. Since the Bauschinger-effect appears only by a reversal of the loading [27], not any surface worksoftening should be found at tensile loading. Therefore and

considering the behaviour of the half width breaths (Fig.1b), identical workhardening curves for surface, transition region and core were taken as a basis for the modelling. The workhardening curves for higher temperatures were determined with the same procedure. Fig. 6b shows the results of the FE-calculations in comparison to the results measured at 25°C and 400°C. For both temperatures at tensile as well as compressive loading an excellent agreement between modelling and measurement exists.
From the comparisons between modelling and measurement it can be concluded that the assumptions are reasonable in respect of the input data of the workhardening curves. This modelling now enables to make additional statements for the properties of the surface layers [25]. At the normalized condition a discrepancy between modelling and measurement occurs at high values of compressive loading stresses (see Fig. 6a), because the calculated residual stresses are always negative, and the measured data at large loadings show a trend towards positive values. These differences can be explained by the generation of barrel-shaped specimens due to compressive deformation, which leads to the development of tensile longitudinal residual stresses on the specimen surface. This behaviour is verified by Fig. 7, where X-ray measured residual stresses are plotted versus the magnitude of plastic strain after compressive loading of an unpeened specimen. For $|\varepsilon_p| \geq 5\%$ the longitudinal residual stresses are about 200 N/mm². Since in the compression tests in connection with the relaxation experiments plastic strains appear up to -3%, it is possible that the specimen shape induces the development of tensile residual stresses at the surface, which are superimposed on the still remaining compressive residual stresses and shift the whole residual stress level in the positive direction. For the quenched and temperered condition this difference does not appear, because on the one hand the deformations are smaller than in the normalized condition and on the other hand, due to the worksoftening of the surface layer, at large compressive loadings tensile residual stresses must be formed on the surface. This behaviour can be explained already qualitatively by the surface-core-composite models, which are presented in [1,2].

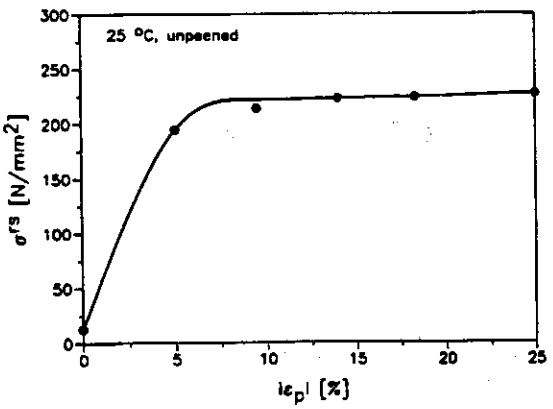

Fig. 7: Residual stress vs. magnitude of plastic strain after compressive deformation of the unpeened normalized condition

From the comparisons between modelling and measurement at increased temperatures a further important statement results. The finding that the presented FE-modelling well describes the residual stress relaxation at higher temperatures, shows that at superimposed thermal and quasistatic loading no additional effects appear, which accelerate the residual stress relaxation. Therefore the residual stress relaxation at higher temperatures can be described for the investigated steel conditions with two

separate processes:
(1) During heating and waiting for temperature compensation of the specimen the residual stress relaxation takes place purely thermally due to dislocation movements in all directions of the activated slip systems.
(2) When bringing up the mechanical loading, the further residual stress relaxation is determined by the corresponding workhardening curves in the individual specimen areas. The residual stress relaxation now results from a stress induced, directed dislocation movement. If the loading time is sufficiently short, the portion of thermal relaxation during mechanical loading can be neglected in the investigated temperature range.

SUMMARY

The residual stress relaxation due to quasistatic loading is influenced at higher temperatures by the dynamic strain ageing, especially at the normalized condition. As a consequence, the trends of the surface residual stresses versus loading stresses lie closely together for all temperatures. At the quenched and tempered condition the effect of dynamic strain ageing is considerably weaker, which produces distinct temperature dependencies of the residual stress - loading stress relationship. While shot peening causes surface workhardening at the normalized condition, a surface worksoftening is observed in the quenched and tempered condition due to the Bauschinger-effect.
The comparison between the measured residual stresses and those calculated with the finite-element method shows a good agreement at both heat treatment conditions and at the investigated temperatures. From this result it can be concluded that for residual stress relaxation due to quasistatic loading at higher temperatures, besides the purely thermal relaxation due to heating and waiting for temperature compensation and quasistatic relaxation, no additional relaxation effect occurs.

ACKNOWLEDGEMENT

The financial support for these investigations by the Deutsche Forschungsgemeinschaft is gratefully acknowledged.

LITERATURE

[1] O. Vöhringer: In "Eigenspannungen, Entstehung- Messung-Bewertung" (Hrsg.: E. Macherauch, V. Hauk).DGM, Oberursel (1983), Bd.1, 49-83
[2] O. Vöhringer: In "Advances in surface treatments" (ed. by A. Niku-Lari). Vol. 4: Int. Guidebook on residual stress, Pergamon Press, New York (1987), 367-396,
[3] J. Hoffmann: Dr.-Ing. Dissertation, Universität Karlsruhe (TH), 1985
[4] J. Hoffmann, B. Scholtes, O. Vöhringer, E. Macherauch: In "Proc. of the Third Int. Conf. on Shot Peening" (ed. by H. Wohlfahrt, R. Kopp, O. Vöhringer). DGM Informationsgesellschaft, Oberursel (1987), 239-246
[5] O. Vöhringer, T. Hirsch, E. Macherauch: In "Titanium Science and Technology"

(ed. by G.Lütjering, U. Zwicker, W. Bunk). DGM Informationsgesellschaft, Oberursel (1985), Vol. 4, 2203-2210
[6] T. Hirsch, O. Vöhringer, E. Macherauch: Härterei-Tech. Mitt. 38 (1983), 229-232
[7] V. Schulze, F. Burgahn, O. Vöhringer, E. Macherauch: Mat..-wiss. u. Werkstofftech. 24 (1993), 258-267
[8] M. Roth: BBC Technische Notiz (26.6.85)
[9] M. Roth: Z. Werkstofftech. 18 (1987), 225-228
[10] U. Schlaak: Dr.-Ing. Dissertation, Universität Bremen, 1988
[11] U. Schlaak, T. Hirsch, P. Mayr: Härterei-Tech. Mitt. 43 (1988), 92-102
[12] F. Wiewecke: Dr.-Ing. Dissertation, Gesamthochschule Kassel-Universität, 1990
[13] F. Wiewecke, H. Wohlfahrt, O. Vöhringer: Härterei-Tech. Mitt. 45 (1990), 293-299
[14] J.M. Potter, R.A. Millard: Advances in X-Ray Analysis (1977), 309-319
[15] N. Masmoudi, L. Castex: In" Proc. of the second Int. Conf. on Residual Stress" (ed. by G. Beck, S. Denis, A. Simon), Elsevier Applied Science, London (1989), 710-715
[16] H. Hanagarth: Dr.-Ing. Dissertation, Universität Karlsruhe (TH), 1989
[17] T. Hirsch, O. Vöhringer, E. Macherauch: Härterei-Tech. Mitt. 43 (1988), 16-20
[18] F. Theobald: Studienarbeit Universität Karlsruhe (TH), 1992
[19] H. Hanagarth, O. Vöhringer, E. Macherauch: In "Proc. of the fourth Int. Conf. on Shot Peening" (ed. by. K. Iida). The Japan Society of Precision Engineering, Tokyo (1990), 327- 336
[20] V. Schulze: Dr.-Ing. Dissertation, Universität Karlsruhe (TH), 1993
[21] D. Kirk: In "Proc. of the third Int. Conf. on Shot Peening" (ed. by H. Wohlfahrt, R. Kopp, O. Vöhringer). DGM Informationsgesellschaft, Oberursel (1987), 213-220
[22] E. Macherauch, P. Müller: Z. f. angew. Physik 7 (1961), 305-312
[23] G. Moore, W.P. Evans: Trans. SAE 66 (1958), 340-345
[24] M.T. Khabou, L. Castex, G. Inglebert, J. Frelat: In "Proc. of the second Int. Conf. on Residual Stress" (ed. by G. Beck, S. Denis, A. Simon). Elsevier Applied Science, London (1989), 619-624
[25] H. Holzapfel: Dr.-Ing. Dissertation, Universität Karlsruhe (TH), 1994
[26] F. Burgahn: Dr.-Ing. Dissertation, Universität Karlsruhe (TH), 1991
[27] B. Scholtes: Dr.-Ing. Dissertation, Universität Karlsruhe (TH), 1980